Impact of ocean color on the maintenance of the Pacific Cold Tongue

W. G. Anderson,[1,2] A. Gnanadesikan,[2] R. Hallberg,[2] J. Dunne,[2] and B. L. Samuels[2]

Received 21 March 2007; revised 26 April 2007; accepted 11 May 2007; published 12 June 2007.

[1] The impact of the penetration length scale of shortwave radiation into the surface ocean is investigated with a fully coupled ocean, atmosphere, land and ice model. Oceanic shortwave radiation penetration is assumed to depend on the chlorophyll concentration. As chlorophyll concentrations increase the distribution of shortwave heating becomes shallower. This change in heat distribution impacts mixed-layer depth. This study shows that removing all chlorophyll from the ocean results in a system that tends strongly towards an El Niño state—suggesting that chlorophyll is implicated in maintenance of the Pacific cold tongue. The regions most responsible for this response are located off-equator and correspond to the oligotrophic gyres. Results from a suite of surface chlorophyll perturbation experiments suggest a potential positive feedback between chlorophyll concentration and a non-local coupled response in the fully coupled ocean-atmosphere system. **Citation:** Anderson, W. G., A. Gnanadesikan, R. Hallberg, J. Dunne, and B. L. Samuels (2007), Impact of ocean color on the maintenance of the Pacific Cold Tongue, *Geophys. Res. Lett.*, *34*, L11609, doi:10.1029/2007GL030100.

1. Introduction

[2] A significant amount of the shortwave radiation hitting the ocean surface is scattered and absorbed at depths considerably shallower than would occur in pure water. In particular, estimated e-folding depths for light with wavelengths between 350nm and 500nm in clear water exceed 50m [*Morel*, 1988]. By contrast, parameterizations of open ocean waters use values of order 20m for penetrating shortwave radiation [*Jerlov*, 1976; *Schneider and Zhu*, 1998] with much shallower e-folding depths in more turbid waters. For many years [*Lewis et al.*, 1990; *Stramska and Dickey*, 1993; *Siegel et al.*, 1995; *Timmermann and Jin*, 2002] it has been speculated that this shallow absorption could alter ocean temperatures and mixed layer depths with impacts on climate. Two principal lines of research have explored this issue. In one the sensitivity of the climate system to changes in the *spatial distribution* of shortwave absorption has been examined in ocean-only [*Sweeney et al.*, 2005; *Manizza et al.*, 2005] and hybrid (simplified atmosphere) coupled models [*Schneider and Zhu*, 1998; *Murtugudde et al.*, 2002; *Ballabrera-Poy et al.*, 2007]. These simulations have shown significant but relatively small impacts from changes in shortwave absorption- with temperature changes of order 0.5°C and- in the hybrid coupled runs- shifts in the structure of ENSO. They distinguish "direct" mechanisms (in which deeper shortwave absorption cools the surface) from indirect mechanisms involved in changing lateral and vertical advection. However, none of these runs allow for the full dynamic and thermodynamic feedbacks of the coupled system to come into play, nor do they examine the control case of an optically clear ocean (having an *e*-folding depth scale for the penetration of shortwave approaching 37 m [*Morel*, 1988]). A second line of research using ocean-only and atmosphere-only models has suggested that such a control case would exhibit larger changes in sea surface temperature [*Nakamoto et al.*, 2001] and that the atmospheric response to these temperature changes could act to enhance them along the equator [*Shell et al.*, 2003].

[3] This work brings these lines of research together, removing shortwave absorption due to dissolved substances using a parameterization that allows deep penetration of blue-green radiation in clear water within a fully coupled climate model. This is important because previous work has not been able to show whether the sum of thermodynamic and dynamic feedbacks is positive or negative. We find that the total impact of shortwave absorption is to shade the cold tongue, resulting in a much enhanced temperature difference between the equatorial zone and extratropics, with important consequences for tropical variability. The mean state of climate with clear ocean water resembles the El Niño state of our simulations with chlorophyll-dependent absorption.

2. Models and Experiments

[4] The ocean model used in this study is the Hallberg Isopycnal Model (HIM) [*Hallberg*, 2005]. HIM is run at 1° resolution in latitude and longitude, with meridional resolution equatorward of 30° becoming progressively finer, such that the meridional resolution is 3/8° at the equator. The ocean mixed layer is represented with a refined bulk mixed layer model [*Hallberg*, 2003]. HIM is coupled to the atmosphere, land and ice components used in the GFDL global coupled climate model [*Delworth et al.*, 2006].

[5] We use the model for shortwave penetration into the water column proposed by *Manizza et al.* [2005] which is based on the data of *Morel* [1988]. The scheme parameterizes shortwave extinction in terms of near-surface chlorophyll-a concentration. It is consistent with the *Morel* [1988] scheme at the lower limit of its validity. The Manizza scheme has a deeper clear-water reference than previous algorithms, resulting in shortwave-induced heating at depths well beyond 100 m. This heating becomes significant when integrated over decadal and larger time-scales.

[6] Two global simulations are run using the simulation protocol for the 1990 control runs with the GFDL coupled climate model [*Delworth et al.*, 2006] in which aerosols and

[1]Program in Atmospheric and Oceanic Sciences, Princeton University, Princeton, New Jersey, USA.
[2]NOAA Geophysical Fluid Dynamics Laboratory, Princeton, New Jersey, USA.

0094-8276/07/2007GL030100$05.00

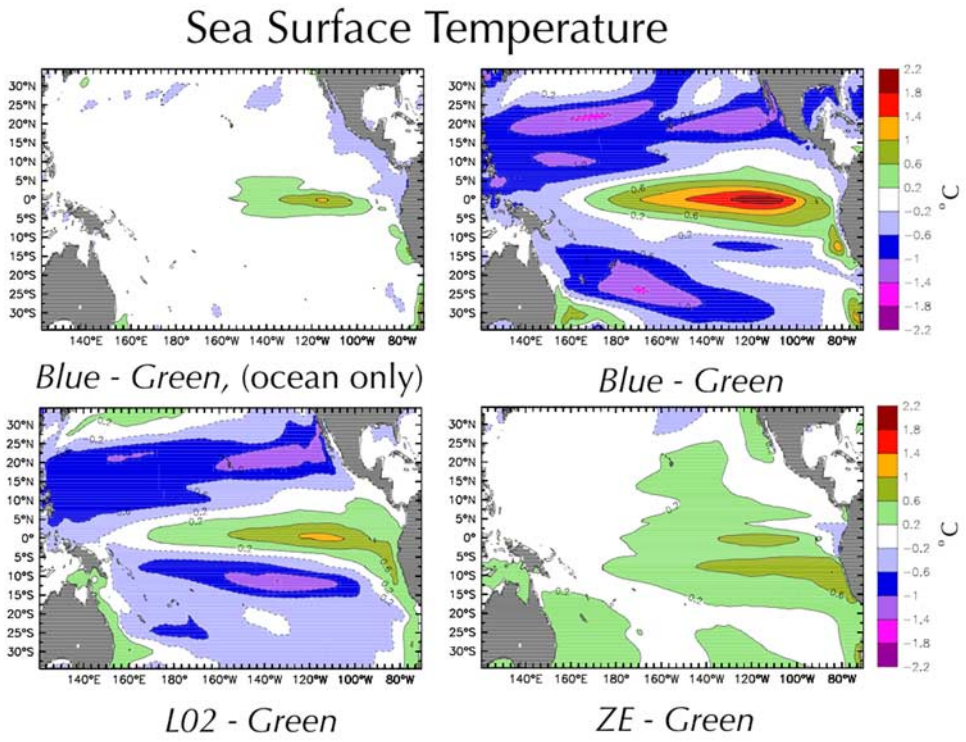

Figure 1. Sea surface temperatures. (top left) The mean for years 10–20 for *Ocean-only-Blue* (zero chlorophyll) minus *Ocean-only-Green* (SeaWiFS chlorophyll). The mean for years 20–60 for (top right) coupled *Blue* minus *Green*, (bottom right) *ZE* (zero chlorophyll, 5°N–5°S), and (bottom left) *L*02 (chlorophyll concentrations below 0.2 mg/m^3 set to zero).

greenhouse gasses were held constant at modern levels. The model performs well on seasonal to interannual timescales in comparison with observations. The model's skill in simulating ENSO is respectable, with realistic Nino3 SST (150°W–90°W; 5°N–5°S) variability and magnitude with a interannual spectral peak near 3–4 years (Figure S1, right, of the auxiliary material).[1]

[7] Initial conditions for all coupled simulations are identical and are based on those described by *Delworth et al.* [2006]. One simulation (*Green*) uses the SeaWiFS monthly composite chlorophyll-a from 1998–2004 (courtesy of the Goddard Earth Sciences Distributed Active Archive Center) to determine the shortwave absorption profile. In a second simulation (*Blue*), chlorophyll-a is set to zero to emulate the absorption profile of optically pure water. These experiments were run for 100 years, long enough to establish surface biases [*Gnanadesikan et al.*, 2006].

[8] In an attempt to isolate coupled response signals, *Blue* and *Green* simulations were also run using climatological atmospheres based on Common Ocean-ice Reference Experiments (CORE) forcing [*Large and Yeager*, 2004]. These will be referred to as "ocean-only" experiments. In comparison to the coupled simulations, the ocean-only simulations converge rapidly to a near steady-state solution. These simulations are only run out to 20 years.

[9] To investigate the importance of equatorial and near equatorial regions, three additional coupled simulations with modification to Pacific chlorophyll monthly mean concentrations are run: one where chlorophyll concentration falling between latitudinal bands 5°N and 5°S in the Pacific are set to zero (*ZE*); a second where chlorophyll concentrations falling below 0.1 mg/m^3 in the Pacific are set to zero (*L*01); and a third where concentrations falling below 0.2 mg/m^3 in the Pacific are set to zero (*L*02) (Figure S2). These simulations are a subset of a larger group of related experiments and due to computational expense are only run for 60 years.

3. Results and Discussion

[10] Our results clearly show the importance of coupling. While the mean SST difference (*Blue* minus *Green*) displays patterns of a weak El Niño in the ocean-only experiments (Figure 1, top left), the magnitude of the pattern is much larger in the coupled runs, exceeding 2°C at the maximum (Figure 1, top right). As expected in a fully coupled system the response was not limited to the ocean temperatures. Time series for common indices of the state of ENSO are shown in Figure 2. These indices show that the mean state of the *Blue* simulation resembles that of an El Niño state as defined by the *Green* simulation. Over the latter 80 years of the *Blue* simulation the La Niña state, as defined by the *Green* simulation, is never entered. Spectral analysis shows a marked drop in both annual and interannual variability when comparing the *Blue* and *Green* simulations (Figure S1).

[11] The pattern of atmospheric response to adding chlorophyll is consistent with previous results [*Shell et al.*, 2003]. The equatorial zonal wind weakens in the runs without chlorophyll. This can be explained, at least in part,

[1] Auxiliary materials are available in the HTML. doi:10.1029/2007GL030100.

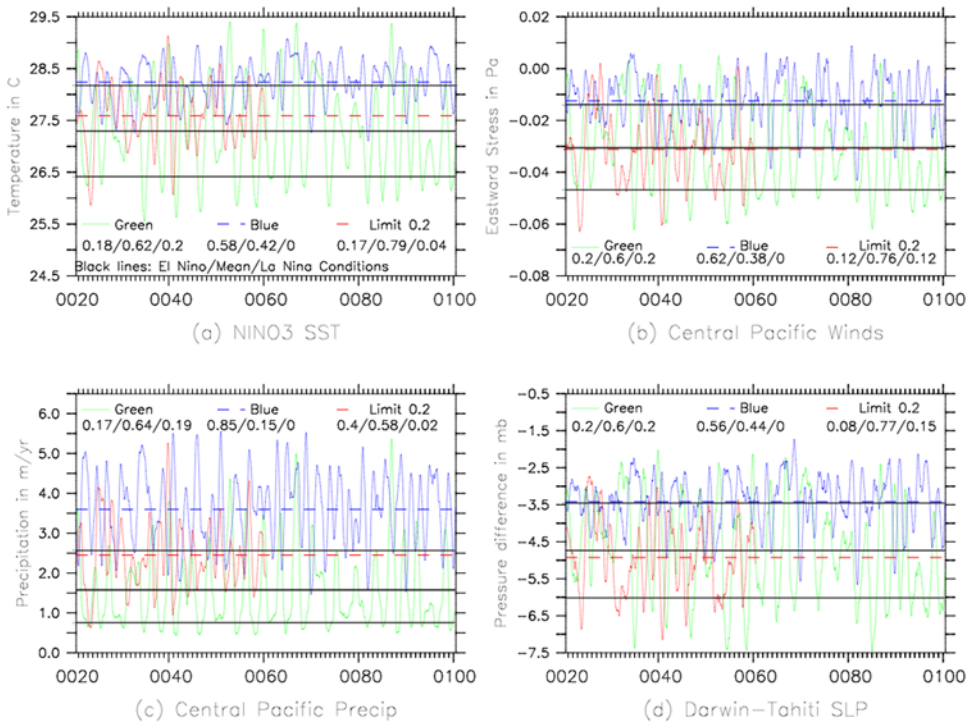

Figure 2. Time series of common ENSO state indices for the *Green* (green), *Blue* (blue) and *L*02 (red) simulations. The indices are: (a) mean annual mean Nino3 SST, (b) central Pacific zonal wind stress, (c) central Pacific precipitation rates, and (d) sea level pressure difference (Darwin minus Tahiti). The solid horizontal black lines indicate the mean and one standard deviation above and one below for the *Green* simulation. The dashed blue line indicates the mean for the *Blue* simulation and the dashed red line for the *LO*2 simulation. The numbers listed within the plots are the fractions of monthly means that fall within El Niño/normal/La Niña conditions as defined by the *Green* simulation.

by the decreased zonal SST gradient set up by the weakened cold tongue in the equatorial Pacific. The warmer SSTs also result in increased equatorial convection and a strengthened Hadley circulation. Large changes in the mean states of precipitation are confined to the tropics. The western Pacific precipitation is shifted westward in *Green* compared to *Blue*, consistent with the changes in the local SSTs (lower temperatures implying less convection). The weaker responses in previous studies can be explained by some combination of the use of a base state in which the ocean is not truly clear (shallower attenuation rates) and the use of single component or partially coupled models resulting in an inability to capture ocean-atmosphere feedbacks and changes in mean state.

[12] The ocean-atmosphere patterns shown in the *Blue* minus *Green* mean state differences develop weakly in the *L*01 (not shown) and strongly in the *L*02 (Figure 1, bottom left). The time series for *L*02 (shown by red lines in Figure 2) all show a reduction in variability when compared to *Green*. However, there are differences between them illustrating the complexity of the coupled system. While *L*02 SST and precipitation rates (Figures 2a and 2c) show a large shift away from La Niña conditions, the temporal mean shows a minimal change in the sea level pressure and central Pacific wind stress. By contrast the wind stress and sea level pressure indices (Figures 2b and 2d) show retreats from both the El Niño and La Niña states as defined by the *Green* simulation.

[13] The zero-ed equator simulation (*ZE*) minus the *Green* shows a weaker and different distribution of warming in than *L*02 (Figure 1, bottom left). The atmosphere in the *ZE* simulation does not behave as it does *Blue* and *L*02. Using the indices shown in Figure 2, the *ZE* simulation (not shown) shows a 25% *increase* in the frequency of cold events to that of *Green* and relatively small changes in the mean atmospheric state. Taken together with the results from *L*02 this implies that the bulk of the differences between *Blue* and *Green* are due to non-local mechanisms.

[14] While the extra-tropical ocean appears to follow the pattern suggested by 1-D analyses [*Lewis et al.*, 1990; *Stramska and Dickey*, 1993] (in which the addition of chlorophyll leads to shoaling of the mixed layer and surface warming), the substantially cooler *Green* tropical Pacific SSTs coincide with little to no local change in mixed-layer depth. Moreover,the *Blue*, *L*01 and *L*02 simulations show warmer tropical Pacific SSTs than the *Green* simulations within the first months. What is the mechanism for these SST changes?

[15] *Sweeney et al.* [2005] suggested that one mechanism for changing equatorial balance was an increase in the meridional transport associated with shoaling mixed layers off-equator. Following their argument, consider the steady linearized off-equatorial momentum balance in the mixed layer

$$-fM_y = \frac{\tau_x}{\rho_o} - \int_{MLD}^{\eta} \frac{1}{\rho_o} \frac{\partial p}{\partial x} dz \qquad (1)$$

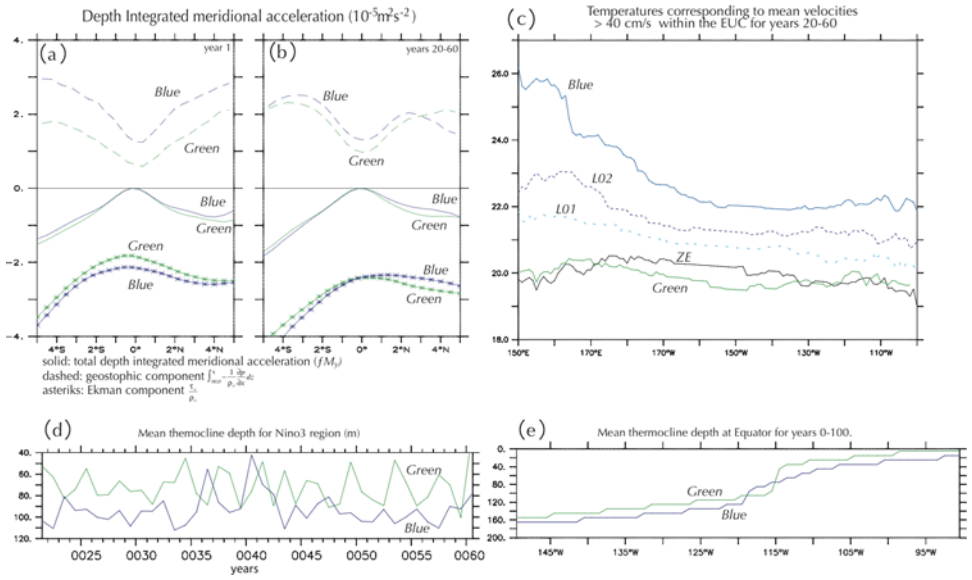

Figure 3. Depth integrated meridional accelerations from equation 1 as calculated by the model. (a) Calculated from annual means of year 1. (b) Years 20–60. (c) Mean temperatures from 2°S to 2°N in waters with an eastward velocity greater than 0.4m/s for years 20–60. (d) The mean Nino3 thermocline depths for years 20–60. (e) The mean thermocline depth at the Equator across the Nino3 region (for years 0–100). The step-like nature of the plots in Figure 3e are due to the remapping of the model climatology to geopotential coordinates.

where $-fM_y$ is depth integrated Coriolis force. Here, f is the Coriolis parameter, M_y is the meridional transport, τ_x is the east-west wind stress, ρ_o is a reference density for seawater, and $\partial p / \partial x$ is the east-west pressure gradient which is integrated from the surface (η) to the base of the mixed layer (*MLD*). By considering the individual terms in this equation one can diagnose possible mechanisms for the increased transport. The terms in equation 1 are calculated from monthly mean averages and plotted in Figure 3. Figure 3a shows the mean values of the terms for the first years of the *Blue* and *Green* coupled simulations. Figure 3b shows the terms calculated for the 20 to 60 year mean. The initial difference in depth integrated Coriolis force (solid lines in Figure 3a) cannot be explained by the difference in the wind stress (asterisks in Figure 3a) as it is of the wrong sign. Significant differences appear in the geostrophic term (second term RHS of equation 1 and dashed lines in Figure 3a) when it is integrated over the MLD. The deeper MLD in the *Blue* simulation results in a stronger equatorward geostrophic acceleration within the mixed layer, reducing upwelling, confirming the mechanism of *Sweeney et al.* [2005]. The coupled atmosphere-ocean response works to amplify the signal and a warm event occurs [*Bjerknes*, 1969]. The mean SST for the Nino3 region rises 1.1 degree Celsius in the *Blue* simulation relative to the *Green*.

[16] However, as the simulations mature the difference in the geostrophic terms diminishes and the difference in poleward acceleration follows the difference in the wind stress terms (Figure 3b). Thus the maintenance of the warm anomaly in the *Blue* run must involve some other mechanism which ensures that the *Blue* system tends to stay in a warm state and prevents it from entering a La Niña. The *L*01 and *L*02 simulations suggest the key is the absence of chlorophyll in the off equatorial regions that would normally (as in the *Green* case) supply cool subsurface waters to the equatorial Pacific regions, shoaling the thermocline. Removing chlorophyll results in these waters receiving more direct heating at depth. If we examine the temperatures of equatorial waters with an eastward velocity exceeding 40 cm/s (Figure 3c) we see that these waters are much warmer in the *Blue* run than in the *Green* run and that a significant fraction of this warming is associated with the *L*02 run, but virtually none with the *ZE* run. This warm water increases the depth of the thermocline, defined as the depth of the maximum vertical temperature gradient, in the Nino3 region (Figure 3d). The slope of the thermocline in the *Blue* run tends to be "flatter" near 115°W, but across the domain is comparable in magnitude to that of *Green*. The *L*01 and *L*02 simulations show similar flattening of the thermocline but not the magnitude of deepening seen in the *Blue* simulation. These results suggest that without the shoaling of the thermocline, termination of the warm event does not occur. While the mechanism is different, the change in thermocline depth required for a permanent El Niño is consistent with that described by *Fedorov et al.* [2006].

4. Conclusions

[17] Our results suggest that previous studies [*Sweeney et al.*, 2005; *Morel*, 1988; *Manizza et al.*, 2005; *Rosati and Miyakoda*, 1988; *Schneider and Zhu*, 1998; *Murtugudde et al.*, 2002; *Nakamoto et al.*, 2001; *Shell et al.*, 2003] may have underestimated the importance of the parameterization of shortwave heating on the maintenance of the Pacific Cold Tongue due to coupled feedbacks. This is consistent with contemporaneous work by *Lengaigne et al.* [2007] in how the tropical Pacific responds to low and high chlorophyll scenarios.

[18] An important corollary is that the shortwave absorption responsible for the cooling and increased upwelling in

the equatorial Pacific is located off-equator. The coupled response to the off-equator chlorophyll suggests possible positive feedbacks when active biology is included. In coarse resolution simulations [*Gnanadesikan et al.*, 2004] up to half of the nutrients used between 10°N–30°N are supplied from the south. The increased upwelling in the equatorial Pacific thus implies an increase in available nutrients for chlorophyll-producing phytoplankton.

[19] The mechanism for the Pacific SST warming seen in our experiments need not be limited to shortwave penetration. Any phenomenon that results in a large enough perturbation in mixed layer depth in the off-equator region could be a viable candidate. Many climate models show a cold tongue bias in the eastern Pacific [*Davey et al.*, 2000]. This could be due to underestimation of off-equatorial shortwave penetration, off-equatorial mixing just below the mixed layer or both. Even though a significant reduction in off-equator chlorophyll is needed to maintain a permanent El Niño, it is possible that changes in chlorophyll could combine with other mechanisms to produce significant effects.

[20] **Acknowledgments.** The authors would like to thank A. Adcroft, M. Manizza, A. Rosati, G. Vecchi, and A. Wittenberg for valuable suggestions and discussions. W.G.A was supported by the NOAA's Geophysical Fluid Dynamics Laboratory through the AOS program at Princeton University.

References

Ballabrera-Poy, J., R. Murtugudde, R. H. Zhang, and A. J. Busalacchi (2007), Coupled ocean-atmosphere response to seasonal modulation of ocean color: Impact on interannual climate simulations in the tropical Pacific, *J. Clim.*, *20*, 353–374.

Bjerknes, J. (1969), Atmospheric teleconnections from the equatorial Pacific, *Mon. Weather Rev.*, *97*, 163–172.

Davey, M. K., et al. (2000), Stoic: A study of coupled model climatology and variability in tropical ocean regions, *Clim. Dyn.*, *18*, 403–420.

Delworth, T. L., et al. (2006), GFDL's CM2 global coupled climate models: part 1. Formulation and simulation characteristics, *J. Clim.*, *19*, 645–674.

Fedorov, A. V., P. S. Dekens, M. McCarthy, A. C. Ravelo, P. B. deMenocal, M. Barreiro, R. C. Pacanowski, and S. G. Philander (2006), The Pliocene paradox (mechanisms for a permanent El Niño), *Science*, *312*, 1485–1489.

Gnanadesikan, A., J. P. Dunne, R. M. Key, K. Matsumoto, J. L. Sarmiento, R. D. Slater, and P. S. Swathi (2004), Oceanic ventilation and biogeochemical cycling: Understanding the physical mechanisms that produce realistic distributions of tracers and productivity, *Global Biogeochem. Cycles*, *18*, GB4010, doi:10.1029/2003GB002097.

Gnanadesikan, A., et al. (2006), GFDL's CM2 global coupled climate models. part 2: The baseline ocean simulation, *J. Clim.*, *19*, 675–697.

Hallberg, R. (2003), The suitability of large-scale ocean models for adapting parameterizations of boundary mixing and a description of a refined bulk mixed layer model, paper presented at 'Aha Huliko'a Hawaiian Winter Workshop, SOEST, Honolulu, Hawaii, 21–24 Jan.

Hallberg, R. (2005), A thermobaric instability of Lagrangian vertical coordinate ocean models, *Ocean Modell.*, *8*, 279–300.

Jerlov, N. G. (1976), *Marine Optics*, *Elsevier Oceanogr. Ser.*, vol. 14, Elsevier, New York.

Large, W., and S. Yeager (2004), Diurnal to decadal global forcing for ocean and sea-ice models: The data sets and flux climatologies, *Tech. Note NCAR/TN-460 + STR*, CGD Div. of the Natl. Cent. for Atmos. Res., Boulder, Colo.

Lengaigne, M., et al. (2007), Influence of the oceanic biology on the tropical Pacific climate in a coupled general circulation model, *Clim. Dyn.*, *28*, 503–516, doi:10.1007/s00382-006-0200-2.

Lewis, M. R., M. E. Carr, G. C. Feldman, W. Esaias, and C. McClain (1990), Influence of penetrating solar radiation on the heat budget of the equatorial Pacific Ocean, *Nature*, *347*, 543–545.

Manizza, M., C. Le Quéré, A. J. Watson, and E. T. Buitenhuis (2005), Bio-optical feedbacks among phytoplankton, upper ocean physics and sea-ice in a global model, *Geophys. Res. Lett.*, *32*, L05603, doi:10.1029/2004GL020778.

Morel, A. (1988), Optical modeling of the upper ocean in relation to its biogenous matter content (case-i waters), *J. Geophys. Res.*, *93*, 10,749–10,768.

Murtugudde, R., J. Beauchamp, C. R. McClain, M. Lewis, and A. Busalacchi (2002), Effects of penetrative radiation on the upper tropical ocean circulation, *J. Clim.*, *15*, 470–486.

Nakamoto, S., S. P. Kumar, J. M. Oberhuber, J. Ishizaka, K. Muneyama, and R. Frouin (2001), Response of the equatorial Pacific to chlorophyll pigment in a mixed layer isopycnal ocean general circulation model, *Geophys. Res. Lett.*, *28*, 2021–2024.

Rosati, A., and K. Miyakoda (1988), A general circulation model for upper ocean simulation, *J. Phys. Oceanogr.*, *18*, 1601–1626.

Schneider, E., and Z. Zhu (1998), Sensitivity of the simulated annual cycle of sea surface temperature in the equatorial Pacific to sunlight parameterization, *J. Clim.*, *11*, 1932–1950.

Shell, K. M., S. Nakamoto, and R. C. Somerville (2003), Atmospheric response to solar radiation absorbed by phytoplankton, *J. Geophys. Res.*, *108*(D15), 4445, doi:10.1029/2003JD003440.

Siegel, D. A., R. R. Bidgare, and Y. Zhou (1995), Solar radiation, phytoplankton pigments and the radiant heating of the equatorial Pacific warm pool, *J. Geophys. Res.*, *100*, 4885–4891.

Stramska, M., and T. D. Dickey (1993), Phytoplankton bloom and the vertical thermal structure of the upper ocean, *J. Mar. Res.*, *51*, 819–842.

Sweeney, C., A. Gnanadesikan, S. Griffies, M. Harrison, A. Rosati, and B. Samuels (2005), Impacts of shortwave penetration depth on large-scale ocean circulation heat transport, *J. Phys. Oceanogr.*, *35*, 1103–1119.

Timmermann, A., and F. Jin (2002), Phytoplankton influences on tropical climate, *Geophys. Res. Lett.*, *39*(23), 2104, doi:10.1029/2002GL015434.

W. G. Anderson, J. Dunne, A. Gnanadesikan, R. Hallberg, and B. L. Samuels, NOAA Geophysical Fluid Dynamics Laboratory, Princeton University Forrestal Campus, 201 Forrestal Road, Princeton, NJ 08540-6649, USA. (whit.anderson@noaa.gov)